Effect of low-intensity pulsed ultrasound on osteogenic differentiation of human induced membrane-derived cells in Masquelet technique

Takase, Kyohei ; Fukui, Tomoaki ; Oe, Keisuke ; Sawauchi, Kenichi ; Yoshikawa, Ryo ; Yamamoto, Yuya ; Hayashi, Shinya ; Matsumoto, Tomoyuk…

(Citation)
Injury,54(6):1444-1450

(Issue Date)
2023-06

(Resource Type)
journal article

(Version)
Version of Record

Injury 54 (2023) 1444–1450

Contents lists available at ScienceDirect

Injury

journal homepage: www.elsevier.com/locate/injury

Effect of low-intensity pulsed ultrasound on osteogenic differentiation of human induced membrane-derived cells in Masquelet technique

Kyohei Takase[a], Tomoaki Fukui[a], Keisuke Oe[a], Kenichi Sawauchi[a], Ryo Yoshikawa[a], Yuya Yamamoto[a], Shinya Hayashi[a], Tomoyuki Matsumoto[a], Ryosuke Kuroda[a], Takahiro Niikura[b,*]

[a] Department of Orthopaedic Surgery, Kobe University Graduate School of Medicine, 7-5-1 Kusunoki-cho, Chuo-ku, Kobe 650-0017, Japan
[b] Department of Orthopaedic Surgery, Hyogo Prefectural Nishinomiya Hospital, 13-9 Rokutanji-cho, Nishinomiya 662-0918, Japan

ARTICLE INFO

Article history:
Accepted 8 April 2023

Keywords:
Low-intensity pulsed ultrasound
Induced membrane
Masquelet technique
Bone defect
Osteogenic differentiation

ABSTRACT

Introduction: The Masquelet technique is a relatively new method for large bone defect treatment. In this technique, grafted bone tissue is used, and after the cement is removed, the induced membrane (IM; that form around the cement spacers placed in the bone defect region) is thought to play an important role in promoting bone formation. On the other hand, low-intensity pulsed ultrasound (LIPUS) is known to promote fracture healing and angiogenesis through mechanical stimulation. This study aimed to investigate the in vitro effects of LIPUS on the osteogenic differentiation of human induced membrane-derived cells (IMCs).

Methods: Seven patients who had been treated using the Masquelet technique were enrolled. The IM was harvested during the second stage of the technique. IMCs were isolated, cultured in growth medium, and then divided into two groups: (1) control group, IMCs cultured in osteogenic medium without LIPUS, and (2) LIPUS group, IMCs cultured in osteogenic medium with LIPUS treatment. Adherent cells from the IM samples were harvested after the first passage and evaluated for cell surface protein expression using immunostaining. A cell proliferation assay was used to count the number of IMCs using a hemocytometer. Osteogenic differentiation capability was assessed using an alkaline phosphatase (ALP) activity assay, Alizarin Red S staining, and real-time reverse transcription-polymerase chain reaction.

Results: Cell surface antigen profiling revealed that the IMCs contained cells positive for the mesenchymal stem cell–related markers CD73, CD90, and CD105. No significant difference in cell numbers was found between the control and LIPUS groups. The ALP activity of IMCs in the LIPUS group was significantly higher than that in the control group on days 7 and 14. Alizarin red S staining intensity was significantly higher in the LIPUS group than in the control group on day 21. Runx2 and VEGF expression was significantly upregulated on days 7 and 14, respectively, compared with levels in the control group.

Conclusion: We demonstrated the significant effect of LIPUS on the osteogenic differentiation of human IMCs. This study indicates that LIPUS can be used as an additional tool for the enhancement of the healing process of the Masquelet technique.

Introduction

Bone transport [1] and vascularized bone grafting [2] have long been used for the reconstruction of critical-sized bone defects associated with severe fractures or debridement for osteomyelitis. The Masquelet technique is a relatively new method that has become widely used as a third treatment option. This technique was first reported by Masquelet et al. in France more than 30 years ago [3]. Since then, many clinical studies have reported favorable outcomes associated with the method [4–6]. Essentially, it is a bone reconstruction technique that can be applied to any bone defect, except lesions on the articular surface, and consists of two stages. In the first stage, a polymethylmethacrylate (PMMA) spacer is placed in the bone defect and left for 6–8 weeks. During this period, a membrane forms around the spacer. In the second stage, the PMMA spacer is removed, and the space surrounded by the induced membrane (IM) is filled with an autologous bone graft. In the Masquelet technique, the IM is thought to play two important roles in promoting bone formation. The first is the mechani-

* Corresponding author.
E-mail address: tniikura@med.kobe-u.ac.jp (T. Niikura).

https://doi.org/10.1016/j.injury.2023.04.004

Table 1
Cell sample data of the seven patients.

Patient	Sex	Age	Affected site	Size of defect	Duration of the spacer in site	Result	Experimental studies performed
1	Male	58	Femur	15 cm	8 w	union	P, A, M, R
2	Male	25	Femur	13 cm	16 w	union	H, P, A, M, R
3	Female	67	Tibia	4 cm	8 w	union	H, P, A, M, R
4	Male	61	Calcaneus	6 cm	12 w	union	P, A, M, R
5	Male	52	Tibia	16 cm	25 w	union	H, P, A, M, R
6	Female	90	Femur	3 cm	9 w	union	P, A, M, R
7	Female	76	Tibia	6 cm	15 w	union	P, A, R

H, histological and immunohistochemical analysis; P, cell proliferation; A, alkaline phosphatase activity assays; M, mineralization; R, real-time reverse transcription-polymerase chain reaction.

cal role that prevents fibrous tissue invasion into the recipient site and resorption of the cancellous bone graft [7,8]. The second is its biological role. Basic experiments have shown that the IM contains mesenchymal stem cells (MSCs) [9,10] and has abundant vascularity [11,12], expression of bone morphogenetic protein (BMP) [13], secretion of growth factors, and bone islands formed with the biomembrane tissue [14,15]. In addition, studies have investigated spacer materials suitable for IM induction in order to improve the mechanical and biological functions of IM [7,16].

Low-intensity pulsed ultrasound (LIPUS) is known to accelerate fracture healing [17,18], and several reports have shown that LIPUS stimulates osteogenic differentiation and angiogenesis in a variety of cells, such as MSCs, in vitro [19,20]. The mechanism by which LIPUS promotes fracture healing has not been fully elucidated; however, several plausible mechanisms have been reported. The nanomotion caused by LIPUS waves translates mechanical signals into biochemical signals through integrin mechanoreceptors in cells [21]. This stimulation leads to the expression of cyclooxygenase 2 (COX-2), which promotes bone remodeling and accelerates fracture healing. In addition, it has been suggested that LIPUS may positively affect vascular endothelial growth factor (VEGF) expression in human osteoblasts in vitro [22].

Based on the findings described above, it is possible that LIPUS acts on MSCs in the IM to cause greater enhancements in osteogenesis. In cases of large bone defects treated by the Masquelet technique, LIPUS would be beneficial with regard to aiding bone regeneration. However, to the best of our knowledge, the effect of LIPUS on IM-derived cells (IMCs) has not been demonstrated.

We hypothesized that LIPUS could direct the differentiation of IMCs into osteoprogenitor cells. In this study, we investigated the in vitro effects of LIPUS on the osteogenic differentiation of IMCs.

Materials and methods

Patient characteristics and surgery

The ethics committee of Kobe University hospital approved this study (No. B200051), and informed consent was obtained from all patients before participation. Seven consecutive patients who were treated using the Masquelet technique at our department between June 2020 and May 2021 were enrolled in this study (Table 1). The patients included four men and three women, with a mean age of 61 years (range, 25–90 years). The IM was harvested in the second stage, during the PMMA cement removal. The size of the harvested IM was 1 cm^2, and sample thickness was as thin as possible to prevent contamination by non-IM tissues, as previously reported [12,13,23].

Isolation and culture of IMCs

IMCs were isolated as previously described for nonunion tissue [24]. Briefly, a small segment (1 cm × 1 cm) of IM was washed, cut into small pieces with a scalpel, and digested at 37 °C for 90 min with 0.2% collagenase type II (Worthington Biochemical Corp, Lakewood, NJ, USA). The cells were cultured in α-modified minimum essential growth medium (Sigma-Aldrich, St. Louis, MO, USA) containing 10% heat-inactivated fetal bovine serum (Sigma-Aldrich), 2 mM L-glutamine (Gibco, Grand Island, NY, USA), and antibiotics, on 10-cm culture dishes. Passage 2 or 3 IMCs were seeded at 3.3×10^4 cells per well in 6-well plates. The cells were incubated in growth medium at 37 °C with 5% humidified CO_2 for 4 days. The growth medium was then changed to an osteogenic medium. The osteogenic medium consisted of a growth medium supplemented with 10 nM dexamethasone (Sigma-Aldrich), 10 mol/L β-glycerophosphate (Sigma-Aldrich), and 50 μg/mL ascorbic acid (Wako, Tokyo, Japan). Each well contained 2 mL of growth medium and osteogenic medium. IMCs were divided into LIPUS and control groups.

LIPUS treatment

A LIPUS exposure device (Teijin Pharma Ltd, Tokyo, Japan) was adapted for use in a 6-well culture plate, as described in previous studies [24–27]. Photographs and schematics of the device are shown in Fig. 1. LIPUS was generated by an array of six lead zirconate titanate transducers fixed to the frame, allowing the array to be positioned correctly in each well of the 6-well culture plate. The culture plate was then placed 5 mm above the array [28]. The LIPUS device was kept in a CO_2 incubator and immersed in a 37 °C water bath to prepare for LIPUS stimulation. The device was set to a 1.5 MHz sine wave with a pulse duration of 200 μs, a repeating pulse at 1 kHz, and a spatial and temporal intensity of 30 mW/cm^2 [29]. The waveform setup was equivalent to the wave conditions of a Sonic Accelerated Fracture Healing System (Teijin Pharma Ltd.). In the LIPUS group, LIPUS was applied daily from the bottom of the culture plate at 37 °C for 20 min.

Histological and immunohistochemical analysis of IMC phenotype

Adherent cells from the IM samples were harvested after the first passage and evaluated for cell surface protein expression using immunostaining. The samples were incubated with fluorescein isothiocyanate-labelled anti-CD73 monoclonal antibody (1:100; 1F-675-T025; Exbio Praha), allophycocyanin-labeled anti-CD90 monoclonal antibody (1:100; 1A-652-T025; Exbio), or phycoerythrin-labeled anti-CD105 monoclonal antibody (1:100; 1P-453-T025; Exbio) at 37 °C for 1 hour. The cells were counterstained with 4′,6-diamidino-2-phenylindole (DAPI) (P36931, Thermo Fisher Scientific), and fluorescent signals were captured via fluorescence spectroscopy using a BZ-X700 microscope (Keyence).

Cell proliferation

A total of 3.3×10^4 IMCs per well were seeded into a six-well plate and cultured for 4 days in growth medium in a stationary

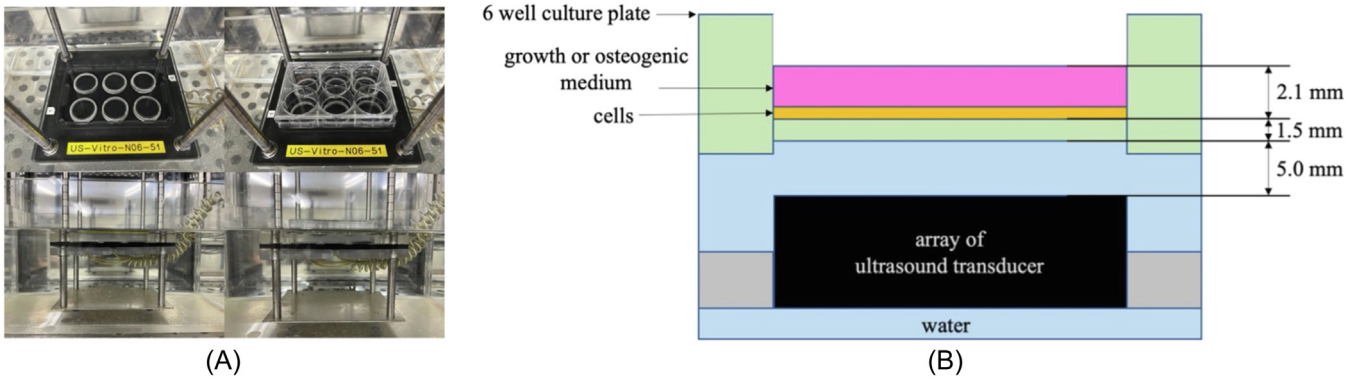

Fig. 1. (a) Low-intensity pulsed ultrasound (LIPUS) exposure system in vitro. (b) Schematic of the LIPUS device. The experimental setup is shown with the key parameters. This Figure was adapted from reference No. 26 Fig. 1.

culture system. LIPUS stimulation was performed for 3, 5, and 7 days. IMCs were detached using 0.05% trypsin-0.02% ethylenediaminetetraacetic acid. Thereafter, 50 μL of IMC sample was mixed with 50 μL of 0.4% trypan blue dye (Gibco BRL) by gently pipetting, and then 20 μL of the mixture was loaded into each chamber of a hemocytometer. Counting was performed in duplicate by one analyst under a 40× objective according to the standard methodology [30].

Osteogenic potential studies

Alkaline phosphatase (ALP) activity assays

Cellular ALP activity was measured on days 7 and 14 using an ALP activity assay. The cell layer from each well was sonicated using a Microson XL2000 ultrasonic cell disruptor (Misonix, Farmingdale, NY, USA) and stored at −80 °C until assay. ALP activity was assayed as the release of p-nitrophenol and was monitored by measuring the optical density at 405 nm using the SensoLyte pNPP Alkaline Phosphatase Assay Kit (AnaSpec Corp, San Jose, CA, USA). The measurement temperature was 37 °C. The protein concentration was standardized using a bicinchoninic acid protein assay kit (Pierce Biotechnology Inc., Rockford, IL, USA). The enzyme activities were normalized with protein concentration and were expressed as absorbance per milligram of protein.

Mineralization

Mineralization is regarded as a functional in vitro endpoint reflecting enhanced cell differentiation in experiments using osteogenic cells. On day 21, the cells were fixed with 95% ethanol for 1 hour at room temperature, and the plate was stained with 1% Alizarin Red S (Hartman Leddon, Philadelphia, PA, USA). The mineralized extracellular matrix was stained red. By incubating the cells in 10% ethylpyridium chloride for 15 min, Alizarin Red S stain was released from the cell matrix, and the amount of dye released was measured as absorbance at 562 nm by spectrophotometry [27].

Expression of osteogenesis and angiogenesis-related genes

Total RNA was extracted from each culture on days 7 and 14 using the RNeasy Mini Kit (Qiagen, Valencia, CA, USA). Total RNA was reverse-transcribed into single-strand complementary DNA using a high-capacity complementary DNA reverse transcription kit (Applied Biosystems, Foster City, CA, USA).

Real-time reverse transcription-polymerase chain reaction (RT-PCR) was performed in triplicate using an Applied Biosystems 7500 real-time PCR system and SYBR Green reagent (Applied Biosystems), according to the recommended protocols. Negative controls included non-RT controls (where total RNA without reverse transcription was used to monitor genomic DNA contamination). The conditions for PCR reactions were as follows: incubation at 95 °C for ten minutes, followed by 40 cycles at 95 °C for 15 s and 60 °C for one minute. All runs were followed by a dissociation curve analysis. Table 2 lists the primer sequences used in the experiments. Each gene's expression level was normalized to that of glyceraldehyde-3-phosphate dehydrogenase (GAPDH), a housekeeping gene, and was presented as the fold change relative to the data of day 0 using the ΔΔCT method (Applied Biosystems) [31].

Table 2
Specific primers for RT-PCR amplifications.

Gene GenBank accession number	Primer sequence (5′ to 3′) (forward/reverse)	Product size (bp)
Runx2	ATGCTTCATTCGCCTCACAAAC	
NM_001024630.4	CCAAAAGAAGTTTTGCTGACATGG	261
OSX	CGGGACTCAACAACTCT	
NM_001173467.3	CCATAGGGGTGTGTCAT	308
OC	GCAAAGGTGCAGCCTTTGTG	
NM_199173.6	GGCTCCCAGCCATTGATACAG	86
BMP2	GGAACGGACATTCGGTCCT	
NM_001200.4	GGAAGCAGCAACGCTAGAAG	162
VEGF	GGGCAGAATCATCACGAAGTG	
NM_001287044.2	ATTGGATGGCAGTAGCTGCG	65
SDF-1	ATGAACGCCAAGGTCGTGG	
NM_001033886.2	CCAGGTACTCCTGAATCCAC	250
GAPDH	CGTCTTCACCACCATGGAGA	
NM_002046.7	CGGCCATCACGCCACAGTTT	300

Runx2, runt-related transcription factor 2; OSX, osterix; OC, osteocalcin; BMP2, bone morphogenetic protein 2; VEGF, vascular endothelial growth factor; SDF-1, stromal cell-derived factor 1; GAPDH, glyceraldehyde-3-phosphate dehydrogenase.

Statistical analysis

Each experiment was performed in triplicate and averaged. All quantitative data are presented as mean ± SE. Statistical comparisons between the groups at each measurement time point were made using the Wilcoxon signed-rank test. Statistical significance was set at $P < 0.05$.

Results

Histological and immunohistochemical analysis of IMC phenotype

IMCs readily expanded in vitro and demonstrated fibroblast-like morphological characteristics (Fig. 2a). The cell surface antigen profile obtained using immunostaining revealed that the IMCs contained cells positive for the MSC-related markers CD73, CD90, and CD105 (Fig. 2b).

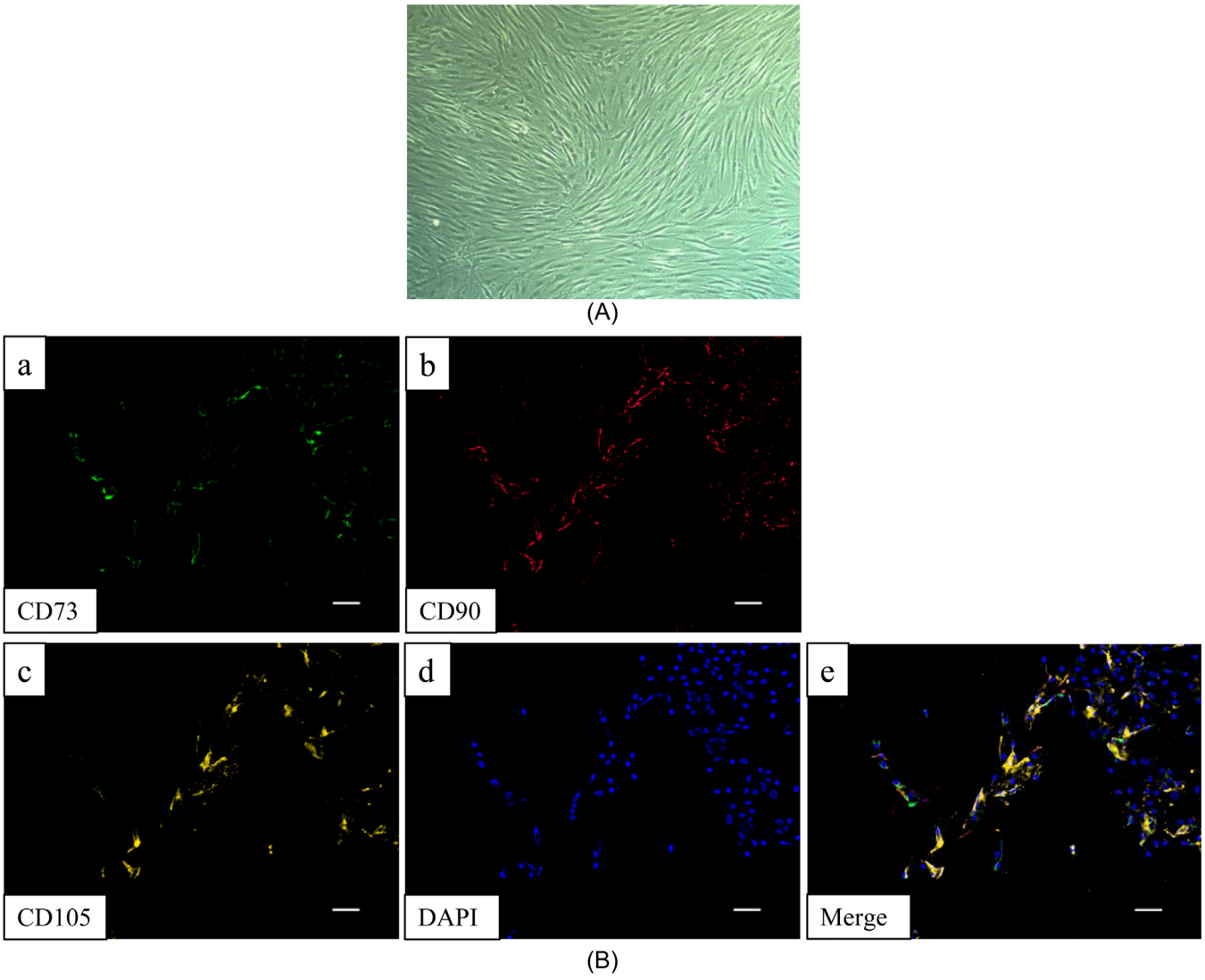

Fig. 2. (A) A microscope image of adherent cells derived from the induced membrane (IM) displaying a fibroblast-like spindle shaped morphology. (B) Representative triple immunostaining for human-CD73 (a), CD90 (b), CD105 (c), DAPI (d), and Merge (e) in induced membrane-derived cells (IMCs). Scale bar: 100 μm.

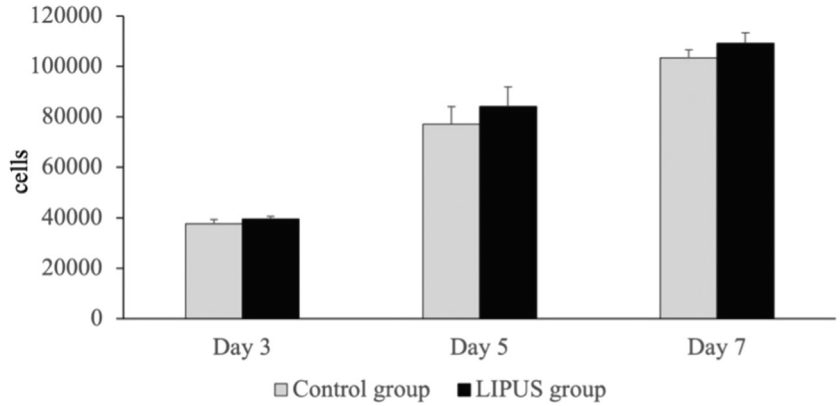

Fig. 3. Proliferation of IMCs relative to the control group on post-treatment days 3, 5, and 7.

Cell proliferation

No significant difference in cell number was observed between the control and LIPUS groups on days 3, 5, and 7 ($P < 0.05$; Fig. 3).

ALP assay

The levels of ALP activity in the LIPUS group on days 7 and 14 were 58.3 ± 10.7 U/ mg protein and 166.6 ± 23.3 U/ mg protein, respectively, compared to those in the control group on days 7 and

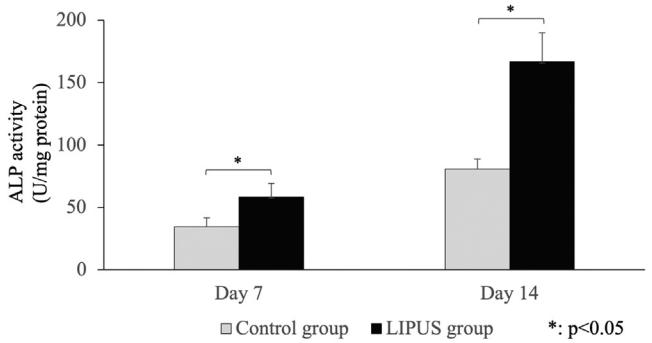

Fig. 4. ALP activity of IMCs on days 7 and 14.

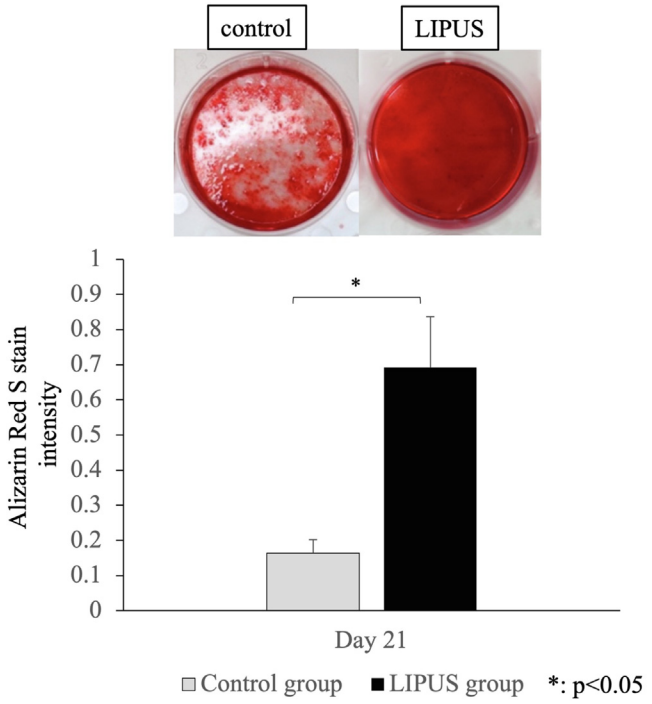

Fig. 5. The Alizarin Red S staining intensity measured as absorbance of LIPUS group and control group at 562 nm on day 21. Photographs: the control cells (**left**), the LIPUS-treated cells (**right**).

14 (34.5 ± 7.1 U/ mg protein and 80.9 ± 7.9 U/ mg protein, respectively). The ALP activity of IMCs in the LIPUS group was significantly higher than that in the control group on days 7 and 14 ($P < 0.05$; Fig. 4).

Mineralization

Fig. 5 demonstrates the Alizarin Red S staining of the LIPUS and control groups on day 21. The photographs clearly show that the LIPUS-treated cells had higher Alizarin Red S staining than the control cells. The intensity of Alizarin Red S staining in the LIPUS group was 0.69 ± 0.15 and was significantly higher than that in the control group ($P < 0.05$; Fig. 5).

Real-time RT-PCR analysis

Fig. 6 ($P < 0.05$) shows the expression of four osteogenesis, angiogenesis, and MSC-related genes. In the LIPUS group, the mRNA expression level of runt-related transcription factor 2 (Runx2) was significantly upregulated compared to that in the control group on day 7. The expression levels of osterix (OSX), osteocalcin (OC), and VEGF in the LIPUS group were significantly higher than those in the control group on day 14. At any time point, there was no significant difference in the mRNA expression levels of bone morphogenetic protein 2 (BMP2) and stromal cell-derived factor 1 (SDF-1) between the two groups.

Discussion

Based on our results of human IM, it was concluded that LIPUS affects IMCs, including MSCs, by enhancing the osteogenic activity thereof. To the best of our knowledge, this is the first study to show that the biological effect of LIPUS on IMCs is significant in vitro.

The Masquelet technique has been widely used to treat large bone defects of 5–26 cm [32]. The average time required for bone union is reported to be 9.1 months [33], and the average bone union rate is 86.0% [34]. Several basic studies on the improvement of this technique have been reported in recent years, including the use of various materials instead of PMMA cement to induce IM and the use of substitute bone to supplement the large number of autografts required [34]. In the current study, we demonstrated for the first time that LIPUS treatment promotes osteogenic differentiation of IMCs, which was proven by upregulation of ALP activity, upregulated expression of osteogenic genes, Runx2, OSX, and OC, and increased calcium mineralization. The present results have important clinical implications in that LIPUS has the potential to further improve the period and rate of bone healing.

At present, the biological functions of IM remain elusive. Several studies have been published on the interaction of cells in autologous bone grafts with IM [35,36]. LIPUS is usually applied to accelerate fracture healing, and the effect is associated with the enhancement of osteogenesis and angiogenesis [26,37]. As previously mentioned, the IM has abundant vascularity and may contribute to bone formation. We have shown that LIPUS enhances VEGF expression in IMCs, indicating that LIPUS could improve the level of blood supply to grafted bone. Furthermore, the MSCs within IMCs are reported to play an important role in osteogenesis [11,23]. Our results demonstrate that IMCs contain cells with cell surface markers similar to those of MSCs. It has been shown that osteogenesis of MSCs can be enhanced with LIPUS by providing local acoustic mechanical stimulation [19], which is consistent with the current results; however, the mechanism by which LIPUS acts on MSCs has not yet been revealed in detail. A small number of studies have indicated that the SDF-1/CXCR4 pathway contributes to fracture healing by inducing MSCs as one of the mechanisms that promote fracture healing in LIPUS [38]; however, there was no significant difference in the expression levels of SDF-1 between the two groups in our study. Further studies are required to elucidate this mechanism. Suzuki et al. reported that LIPUS treatment increased the expression of BMP2 in rat osteoblasts [39]. Several studies have reported the expression of the BMP2 protein in human IM [15,23]. The present results demonstrated that LIPUS tended to upregulate the expression level of BMP2 in human IM, although the difference was not significant. BMP2 is known to play an important role in osteoblast differentiation through the activation of the Smad signaling pathway [40], and it is possible that endogenous BMP2 upregulation may have influenced the osteogenic differentiation of IMCs.

LIPUS treatment had no significant effect on IMC proliferation on days 3, 5, and 7, indicating that LIPUS did not affect cell proliferation. Some studies have shown that LIPUS mainly affects the differentiation rather than proliferation of human nonunion tissue-derived cells and human MSCs [24,41]. Our results suggest that LIPUS similarly affects IMC cell differentiation rather than cell proliferation, and may play a regulatory role in IMC osteogenic differentiation.

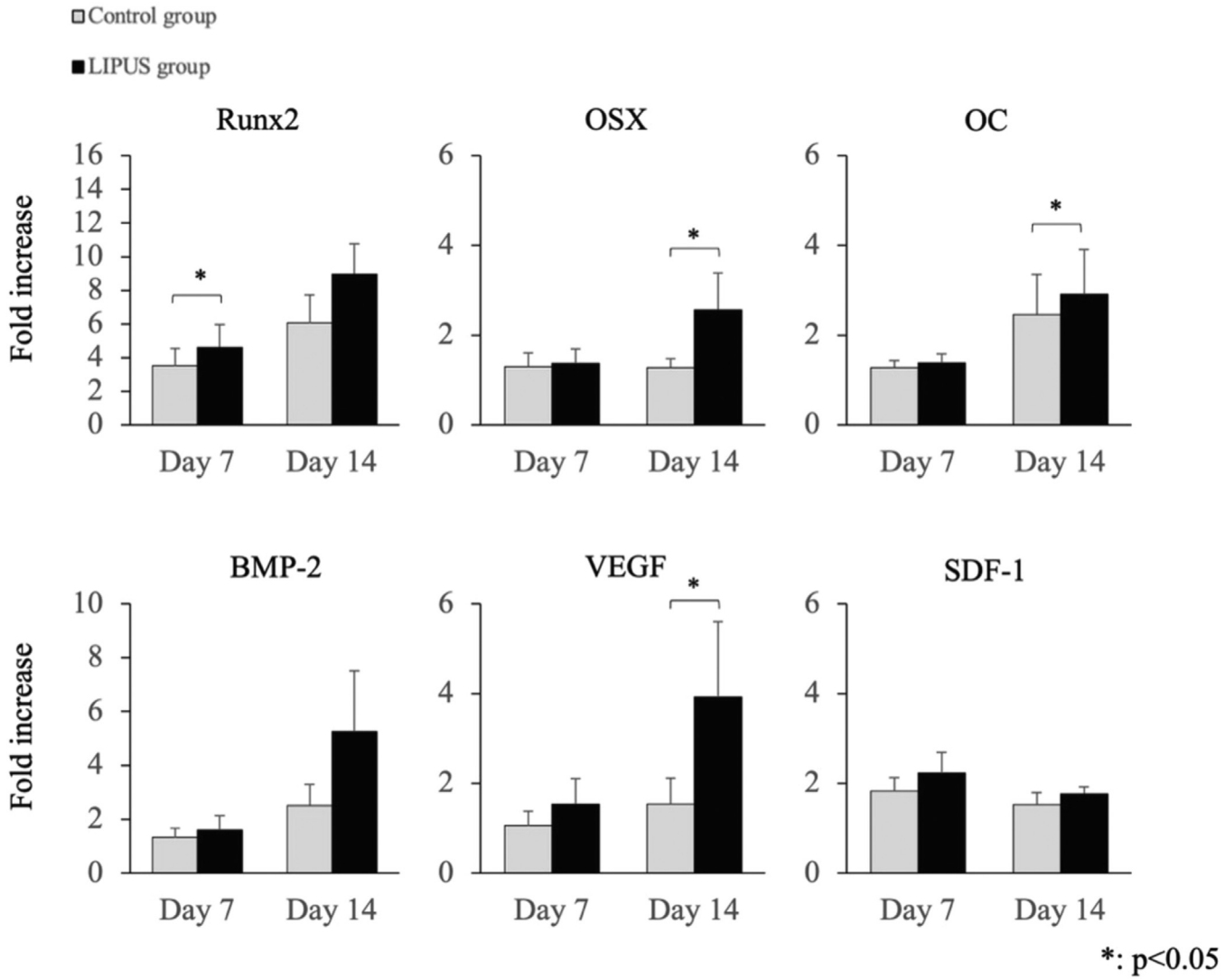

Fig. 6. Real-time RT-PCR analysis of gene expression of Runx2, OSX, OC, BMP-2, VEGF, and SDF-1 on days 7 and 14.

This study had one clear limitation in that we focused on the effect of LIPUS on IMCs; however, further experiments regarding the effects of LIPUS on IM tissue and bone grafts surrounded by the IM would be required, especially with regard to the use of LIPUS with the Masquelet technique in a clinical setting.

In conclusion, we demonstrated the significant effect of LIPUS on the osteogenic differentiation of human IMCs. This study indicates that LIPUS can be used as an additional tool for the enhancement of the healing process in the Masquelet technique.

Funding

This research did not receive any specific grant from funding agencies in the public, commercial, or not-for-profit sectors.

Ethics Approval

All protocols of this study were approved by the Ethics Committee of Kobe University Graduate School of Medicine (Kobe, Japan) (approval number: B200051).

Declaration of Competing Interest

None.

Acknowledgments

The authors thank Ms. Kyoko Tanaka, Maya Yasuda, and Minako Nagata (Department of Orthopaedic Surgery, Kobe University Graduate School of Medicine, Kobe, Japan) for their technical assistance.

References

[1] Aktuglu K, Erol K, Vahabi A. Ilizarov bone transport and treatment of critical-sized tibial bone defects: a narrative review. J Orthop Traumatol 2019;20:22. doi:10.1186/s10195-019-0527-1.
[2] Cano-Luís P, Andrés-Cano P, Ricón-Recarey FJ, Giráldez-Sánchez MA. Treatment of posttraumatic bone defects of the forearm with vascularized fibular grafts. Follow up after fourteen years. Injury 2018;49(Suppl 2):S27–35. doi:10.1016/j.injury.2018.07.021.
[3] Masquelet AC, Fitoussi F, Begue T, Muller GP. Reconstruction of the long bones by the induced membrane and spongy autograft. Ann Chir Plast Esthet 2000;45:346–53.
[4] Masquelet AC, Begue T. The concept of induced membrane for reconstruction of long bone defects. Orthop Clin North Am 2010;41:27–37 table of contents. doi:10.1016/j.ocl.2009.07.011.
[5] Chong KW, Woon CYL, Wong MK. Induced membranes-a staged technique of bone-grafting for segmental bone loss: surgical technique. J Bone Joint Surg Am 2011;93(Suppl 1):85–91. doi:10.2106/JBJS.J.01251.
[6] Masquelet AC, Kishi T, Benko PE. Very long-term results of post-traumatic bone defect reconstruction by the induced membrane technique. Orthop Traumatol Surg Res 2019;105:159–66. doi:10.1016/j.otsr.2018.11.012.
[7] Gaio N, Martino A, Toth Z, Watson JT, Nicolaou D, McBride-Gagyi S. Masquelet Technique: the effect of altering implant material and topography on membrane matrix composition, mechanical and barrier properties in a rat defect model. J Biomech 2018;72:53–62. doi:10.1016/j.jbiomech.2018.02.026.

[8] Dimitriou R, Mataliotakis GI, Calori GM, Giannoudis PV. The role of barrier membranes for guided bone regeneration and restoration of large bone defects: current experimental and clinical evidence. BMC Med 2012;10:81. doi:10.1186/1741-7015-10-81.
[9] Gruber HE, Riley FE, Hoelscher GL, Bayoumi EM, Ingram JA, Ramp WK, et al. Osteogenic and chondrogenic potential of biomembrane cells from the PMMA-segmental defect rat model. J Orthop Res 2012;30:1198–212. doi:10.1002/jor.22047.
[10] Henrich D, Seebach C, Nau C, Basan S, Relja B, Wilhelm K, et al. Establishment and characterization of the Masquelet induced membrane technique in a rat femur critical-sized defect model. J Tissue Eng Regen Med 2016;10:E382–96. doi:10.1002/term.1826.
[11] Aho OM, Lehenkari P, Ristiniemi J, Lehtonen S, Risteli J, Leskelä HV. The mechanism of action of induced membranes in bone repair. J Bone Joint Surg Am 2013;95:597–604. doi:10.2106/JBJS.L.00310.
[12] Niikura T, Jimbo N, Komatsu M, Oe K, Fukui T, Matsumoto T, et al. Histological analysis of induced membranes in patients whose bone defects were treated with the Masquelet technique to identify factors affecting the vascularity of induced membranes. J Orthop Surg Res 2021;16:248. doi:10.1186/s13018-021-02404-7.
[13] Niikura T, Oda T, Jimbo N, Komatsu M, Oe K, Fukui T, et al. Immunohistochemical analysis revealed the expression of bone morphogenetic proteins-4, 6, 7, and 9 in human induced membrane samples treated with the Masquelet technique. J Orthop Surg Res 2022;17:29. doi:10.1186/s13018-022-02922-y.
[14] Pelissier P, Masquelet AC, Bareille R, Pelissier SM, Amedee J. Induced membranes secrete growth factors including vascular and osteoinductive factors and could stimulate bone regeneration. J Orthop Res 2004;22:73–9. doi:10.1016/S0736-0266(03)00165-7.
[15] Gruber HE, Ode G, Hoelscher G, Ingram J, Bethea S, Bosse MJ. Osteogenic, stem cell and molecular characterisation of the human induced membrane from extremity bone defects. Bone Joint Res 2016;5:106–15. doi:10.1302/2046-3758.54.2000483.
[16] Franz S, Rammelt S, Scharnweber D, Simon JC. Immune responses to implants - a review of the implications for the design of immunomodulatory biomaterials. Biomaterials 2011;32:6692–709. doi:10.1016/j.biomaterials.2011.05.078.
[17] Rubin C, Bolander M, Ryaby JP, Hadjiargyrou M. The use of low-intensity ultrasound to accelerate the healing of fractures. J Bone Joint Surg Am 2001;83:259–70. doi:10.2106/00004623-200102000-00015.
[18] Griffin XL, Costello I, Costa ML. The role of low intensity pulsed ultrasound therapy in the management of acute fractures: a systematic review. J Trauma 2008;65:1446–52. doi:10.1097/TA.0b013e318185e222.
[19] Sant'Anna EF, Leven RM, Virdi AS, Sumner DR. Effect of low intensity pulsed ultrasound and BMP-2 on rat bone marrow stromal cell gene expression. J Orthop Res 2005;23:646–52. doi:10.1016/j.orthres.2004.09.007.
[20] Barzelai S, Sharabani-Yosef O, Holbova R, Castel D, Walden R, Engelberg S, et al. Low-intensity ultrasound induces angiogenesis in rat hind-limb ischemia. Ultrasound Med Biol 2006;32:139–45. doi:10.1016/j.ultrasmedbio.2005.08.010.
[21] Harrison A, Lin S, Pounder N, Mikuni-Takagaki Y. Mode & mechanism of low intensity pulsed ultrasound (LIPUS) in fracture repair. Ultrasonics 2016;70:45–52. doi:10.1016/j.ultras.2016.03.016.
[22] Leung KS, Cheung WH, Zhang C, Lee KM, Lo HK. Low intensity pulsed ultrasound stimulates osteogenic activity of human periosteal cells. Clin Orthop Relat Res 2004;418:253–9. doi:10.1097/00003086-200401000-00044.
[23] Cuthbert RJ, Churchman SM, Tan HB, McGonagle D, Jones E, Giannoudis PV. Induced periosteum a complex cellular scaffold for the treatment of large bone defects. Bone 2013;57:484–92. doi:10.1016/j.bone.2013.08.009.
[24] Koga T, Lee SY, Niikura T, Koh A, Dogaki Y, Okumachi E, et al. Effect of low- intensity pulsed ultrasound on bone morphogenetic protein 7-induced osteogenic differentiation of human nonunion tissue-derived cells in vitro. J Ultrasound Med 2013;32:915–22. doi:10.7863/ultra.32.6.915.
[25] Lee SY, Koh A, Niikura T, Oe K, Koga T, Dogaki Y, et al. Low-intensity pulsed ultrasound enhances BMP-7-induced osteogenic differentiation of human fracture hematoma-derived progenitor cells in vitro. J Orthop Trauma 2013;27:29–33. doi:10.1097/BOT.0b013e3182519492.
[26] Hasegawa T, Miwa M, Sakai Y, Niikura T, Kurosaka M, Komori T. Osteogenic activity of human fracture haematoma-derived progenitor cells is stimulated by low-intensity pulsed ultrasound in vitro. J Bone Joint Surg Br 2009;91:264–70. doi:10.1302/0301-620X.91B2.20827.
[27] Sawauchi K, Fukui T, Oe K, Kumabe Y, Oda T, Yoshikawa R, et al. Low-intensity pulsed ultrasound promotes osteogenic differentiation of reamer-irrigator-aspirator graft-derived cells in vitro. Ultrasound Med Biol 2022;48:313–22. doi:10.1016/j.ultrasmedbio.2021.10.006.
[28] Iwabuchi S, Ito M, Hata J, Chikanishi T, Azuma Y, Haro H. In vitro evaluation of low-intensity pulsed ultrasound in herniated disc resorption. Biomaterials 2005;26:7104–14. doi:10.1016/j.biomaterials.2005.05.004.
[29] Heckman JD, Ryaby JP, McCabe J, Frey JJ, Kilcoyne RF. Acceleration of tibial fracture-healing by non-invasive, low-intensity pulsed ultrasound. J Bone Joint Surg Am 1994;76:26–34. doi:10.2106/00004623-199401000-00004.
[30] Louis KS, Siegel AC. Cell viability analysis using trypan blue: manual and automated methods. Methods Mol Biol 2011;740:7–12. doi:10.1007/978-1-61779-108-6_2.
[31] Livak KJ, Schmittgen TD. Analysis of relative gene expression data using real-time quantitative PCR and the 2(-Delta Delta C(T)) method. Methods 2001;25:402–8. doi:10.1006/meth.2001.1262.
[32] Moghaddam A, Zietzschmann S, Bruckner T, Schmidmaier G. Treatment of atrophic tibia non-unions according to "diamond concept": results of one- and two-step treatment. Injury 2015;46:S39–50. doi:10.1016/S0020-1383(15)30017-6.
[33] Careri S, Vitiello R, Oliva MS, Ziranu A, Maccauro G, Perisano C. Masquelet technique and osteomyelitis: innovations and literature review. Eur Rev Med Pharmacol Sci 2019;23:210–16. doi:10.26355/eurrev_201904_17495.
[34] Masquelet AC, Kanakaris NK, Obert L, Stafford P, Giannoudis PV. Bone repair using the masquelet technique. J Bone Joint Surg Am 2019;101:1024–36. http://doi.org/10.2106/JBJS.18.00842.
[35] Wang X, Wei F, Luo F, Huang K, Xie Z. Induction of granulation tissue for the secretion of growth factors and the promotion of bone defect repair. J Orthop Surg Res 2015;10:147. http://doi.org/10.1186/s13018-015-0287-4.
[36] Tang Q, Tong M, Zheng G, Shen L, Shang P, Liu H. Masquelet's induced membrane promotes the osteogenic differentiation of bone marrow mesenchymal stem cells by activating the Smad and MAPK pathways. Am J Transl Res 2018;10:1211–19.
[37] Coords M, Breitbart E, Paglia D, Kappy N, Gandhi A, Cottrell J, et al. The effects of low-intensity pulsed ultrasound upon diabetic fracture healing. J Orthop Res 2011;29:181–8. http://doi.org/10.1002/jor.21223.
[38] Wei FY, Leung KS, Li G, Qin J, Chow SK, Huang S, et al. Low intensity pulsed ultrasound enhanced mesenchymal stem cell recruitment through stromal derived factor-1 signaling in fracture healing. PLoS ONE 2014;9. e106722 http://doi.org/10.1371/journal.pone.0106722 .
[39] Suzuki A, Takayama T, Suzuki N, Sato M, Fukuda T, Ito K. Daily low-intensity pulsed ultrasound-mediated osteogenic differentiation in rat osteoblasts. Acta Biochim Biophys Sin (Shanghai) 2009;41:108–15. http://doi.org/10.1093/abbs/gmn012.
[40] Fujii M, Takeda K, Imamura T, Aoki H, Sampath TK, Enomoto S, et al. Roles of bone morphogenetic protein type I receptors and Smad proteins in osteoblast and chondroblast differentiation. Mol Biol Cell 1999;10:3801–13. http://doi.org/10.1091/mbc.10.11.3801.
[41] Noriega S, Mamedov T, Turner JA, Subramanian A. Intermittent applications of continuous ultrasound on the viability, proliferation, morphology, and matrix production of chondrocytes in 3D matrices. Tissue Eng 2007;13:611–18. http://doi.org/10.1089/ten.2006.0130.